Aluminum Alkyl Complexes Containing Guanidinate Ligands

Sarah L. Aeilts, Martyn P. Coles, Dale C. Swenson, and Richard F. Jordan*

Department of Chemistry, The University of Iowa, Iowa City, Iowa 52242

Victor G. Young, Jr.

Department of Chemistry, The University of Minnesota, Minneapolis, Minnesota 55455

Received March 25, 1998

The synthesis and structures of new aluminum complexes incorporating guanidinate ligands ($R_2NC(NR'_2)^-$) are described. The reaction of ^{i}PrN═C═N^{i}Pr with $LiNR_2$ reagents yields $Li[R_2NC(N^iPr)_2]$ guanidinate salts, which are reacted in situ with $AlCl_3$ or $AlMe_2Cl$ to afford $\{R_2NC(N^iPr)_2\}AlCl_2$ (**1a**, R = Me; **1b**, R = Et; **1c**, R = ^{i}Pr; **1d**, R = $SiMe_3$) or $\{R_2NC(N^iPr)_2\}AlMe_2$ (**2a**, R = Me; **2b**, R = Et; **2c**, R = ^{i}Pr), respectively. The reaction of 1,3,4,6,7,8-hexahydro-2*H*-pyrimido[1,2-*a*]pyrimidine (hppH) with $AlMe_3$ generates $\{(\mu\text{-hpp})AlMe_2\}_2$ (**3**). Complexes **1a**, **1d**, and **3** have been characterized by X-ray crystallography. **1a** and **1d** adopt monomeric structures with symmetric chelated bidentate guanidinate ligands. Delocalization of the $-NR_2$ lone pair into the chelate ring is important for **1a** but not for **1d**, due to N−Si π-bonding and steric crowding. The bicyclic structure of the hpp^- ligand enforces a dimeric μ-hpp^- structure for **3**.

Introduction

Alkyl abstraction from aluminum amidinate dialkyl complexes ($\{RC(NR'_2)\}AlR_2$) yields cationic aluminum alkyls **A**−**C** (Chart 1), the structures of which depend on the presence or absence of potential donor ligands L, the coordinating ability of the counterion A^-, and the steric properties of the $\{RC(NR'_2)\}AlR_2$ starting compound.[1] In particular, the use of bulky amidinate ligands, in which steric interactions between the C−R and N−R′ substituents decrease the R′−N−Al angle (and increase the amidinate cone angle), disfavors the formation of dinuclear cations **A**.[2] We have shown that $\{RC(NR'_2)\}AlR^+$ species catalyze the polymerization of ethylene to high molecular weight polyethylene.[1] We are interested in developing the chemistry of new aluminum alkyls containing other anionic, bidentate ancillary ligands which may provide broader possibilities for tuning the steric and electronic properties and ultimately the reactivity properties of cationic aluminum alkyls. Here, we describe initial studies of neutral aluminum compounds containing guanidinate ligands ($R_2NC(NR'_2)^-$, Chart 2).

Guanidinate ligands (Chart 2) are related to amidinates by substitution of the central C−R substituent by an amino group.[3,4] Recent studies have shown that guanidinates can coordinate to transition and main-group metals in a variety of ways, including (i) as bridging ligands, e.g., in $\{(terpyridine)Pt\}_2(\mu\text{-}\eta^2\text{-}H_2NC(NH)_2\}$ and $Mo_2\{\mu\text{-}\eta^2\text{-}HPhNC(NPh)_2\}_4^{n+}$ (n = 0,1),[5,6] (ii) as unsymmetrical bidentate chelating ligands, e.g., in $Sb\{H^iPrNC(N^iPr)_2\}\{^iPrC(N^iPr)_2\}$ and $Mg\{^iPr_2NC(N^iPr)_2\}_2(THF)$,[7,8] and (iii) as symmetrical bidentate chelating ligands, e.g., in $Cp^*\{HPhNC(NPh)_2\}RhCl$, $(\eta^6\text{-}p\text{-}C_6H_4Me^iPr)\{HPhNC(NPh)_2\}RuCl$, and $Cp\{HRNC(NPh)_2\}Mo(CO)_2$ (R = H, Ph).[9,10]

Chart 1

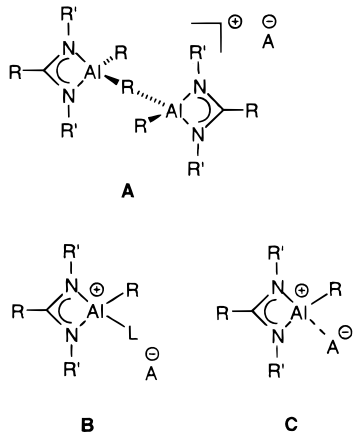

(1) Coles, M. P.; Jordan, R. F. *J. Am. Chem. Soc.* **1997**, *119*, 8125.
(2) Coles, M. P.; Swenson, D. C.; Jordan, R. F.; Young, V. G., Jr. *Organometallics* **1997**, *16*, 5183.
(3) (a) In the literature, $R_2NC(NR'_2)^-$ ligands have been referred to as guanidinate, guanidino, guanidine, and guanidine anion ligands. (b) Wade has described aluminum alkyl adducts of 1,1,3,3-tetramethylguanidine, i.e., $AlR_3\{N(H)═C(NMe_2)_2\}$ (R = Me, Et) and dimeric compounds containing the deprotonated form of this ligand, i.e., $[AlX_2\{\mu\text{-}N═C(NMe_2)_2\}]_2$ (X = Me, Et, Cl). The $(Me_2N)_2C═N^-$ ligand in the latter compounds is isomeric to the guanidinate ligands described here, see: Snaith, R.; Wade, K.; Wyatt, B. K. *J. Chem. Soc. A* **1970**, 380.
(4) Mehrotra, R. C. *Comprehensive Coordination Chemistry*; Wilkinson, G., Ed.; Pergamon: Oxford, 1987; Vol 2, pp 269−291.
(5) (a) Ratilla, E. M. A.; Scott, B. K.; Moxness, M. S.; Kostic, N. M. *Inorg. Chem.* **1990**, *29*, 918. (b) Yip, H. K.; Che, C. M.; Zhou, Z. Y.; Mak, T. C. W. *J. Chem. Soc., Chem. Commun.* **1992**, 1369.
(6) Bailey, P. J.; Bone, S. F.; Mitchell, L. A.; Parsons, S.; Taylor, K. J.; Yellowlees, L. J. *Inorg. Chem.* **1997**, *36*, 867.
(7) Bailey, P. J.; Gould, R. O.; Harmer, C. N.; Pace, S.; Steiner, A.; Wright, D. S. *J. Chem. Soc., Chem. Commun.* **1997**, 1161.
(8) Srinivas, B.; Chang, C. C.; Chen, C. H.; Chiang, M. Y.; Chen, I. T.; Wang, Y.; Lee, G. H. *J. Chem. Soc., Dalton Trans.* **1997**, 957.

S0276-7333(98)00223-4 CCC: $15.00
Publication on Web 06/24/1998

Chart 2

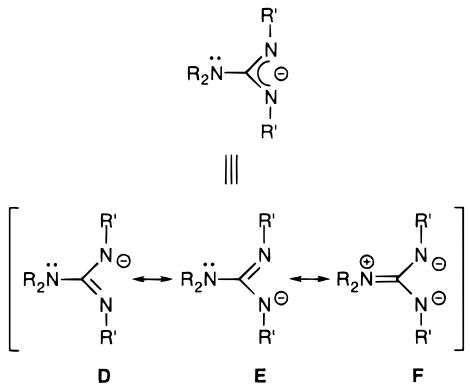

Chart 3

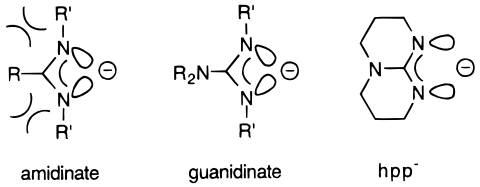

The three principal resonance structures for a guanidinate anion, **D**−**F**, are shown in Chart 2. Structure **F**, which has no counterpart in amidinate ligands, is noteworthy because the delocalization of the $-NR_2$ lone pair into the π system increases the charge on the nitrogen-donor atoms. Delocalization of this type should strengthen guanidinate−metal bonding in complexes of high oxidation state or electron-deficient metals. On the other hand, steric crowding between the NR_2 and NR' groups or N−R π-bonding will disfavor **F**. Therefore, it may be possible to control the donor properties of guanidinate ligands by varying the R and R′ substituents.

One factor which influences the bonding mode (chelating versus bridging) of amidinate ligands is steric crowding within the amidinate ligand itself.[11] As illustrated in Chart 3, steric crowding between the C−R and N−R′ groups causes the nitrogen σ-donor orbitals to project more toward the center of the amidinate "mouth" and favors a chelating bonding mode. Thus, for example, [{μ-MeC(NMe)$_2$}AlMe$_2$]$_2$ adopts a dinuclear structure with bridging amidinate ligands,[12] while {MeC(NCy)$_2$}AlMe$_2$ and {^{t}BuC(NCy)$_2$}AlMe$_2$ are monomeric.[2] Similar steric control of the bonding preferences of guanidinate ligands may be complicated by the electronic issues discussed above. However, one guanidinate ligand which is predisposed to coordinate in a bridging mode is the bicyclic 1,3,4,6,7,8-hexahydro-2*H*-pyrimido[1,2-*a*]pyrimidinato anion (hpp$^-$, Chart 3). In this case, the N−*R*′ groups are effectively "tied back" so that the nitrogen sp^2-donor orbitals project in parallel directions. Several dinuclear metal−metal-bonded compounds incorporating hpp$^-$ have been reported recently,

Scheme 1

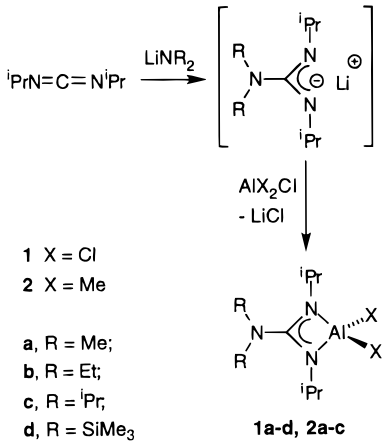

including Ru$_2$(hpp)$_4$Cl$_2$, Nb$_2$(hpp)$_4$, and Mo$_2$(hpp)$_4^{n+}$ (n = 0, 2).[13,14,15]

Results and Discussion

Synthesis of Aluminum Guanidinate Complexes. The reaction of diisopropylcarbodiimide (^{i}PrN=C=N^{i}Pr) with LiNR$_2$ reagents (R = Me, Et, ^{i}Pr, SiMe$_3$) generates lithium guanidinates Li[R$_2$NC(N^{i}Pr)$_2$].[16] These salts were not isolated but rather were reacted with AlCl$_3$ or AlMe$_2$Cl in situ to afford the complexes {R$_2$NC(N^{i}Pr)$_2$}AlCl$_2$ (**1a**, R = Me; **1b**, R = Et; **1c**, R = ^{i}Pr; **1d**, R = SiMe$_3$) or {R$_2$NC(N^{i}Pr)$_2$}AlMe$_2$ (**2a**, R = Me; **2b**, R = Et; **2c**, R = ^{i}Pr), respectively (Scheme 1). The dichloride complexes **1a**−**d** are isolated as white or pale yellow crystals by recrystallization from pentane or toluene. The dimethyl complexes **2a**−**c** are isolated as low melting point solids and can be purified by sublimation (70 °C). The ^{1}H and ^{13}C NMR spectra of **1a**−**d** and **2a**−**c** are consistent with C_{2v}-symmetric structures. The ^{13}C NMR spectra of **2a**−**c** contain high-field Al−*C* resonances which are broadened due to the ^{27}Al quadrupole and exhibit low $^1J_{CH}$ values (110−115 Hz). Mass spectral data for **1a**−**d** and **2a**−**c** are consistent with monomeric structures.

The reaction of hppH and AlMe$_3$ affords {(μ-hpp)-AlMe$_2$}$_2$ (**3**, eq 1). Compound **3** is insoluble in hydro-

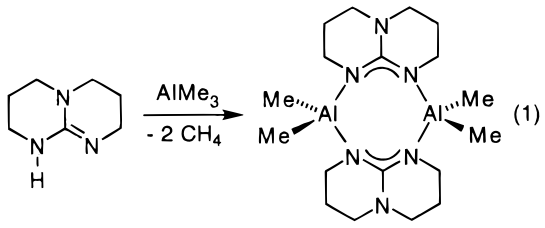

3

carbon solvents, CH_3CN and CH_2Cl_2, but may be purified by recrystallization from hot THF as colorless

(9) Bailey, P. J.; Mitchell, L. A.; Parsons, S. *J. Chem. Soc., Dalton Trans.* **1996**, 2839.
(10) Maia, J. R. d. S.; Gazard, P. A.; Kilner, M.; Batsanov, A. S.; Howard, J. A. K. *J. Chem. Soc., Dalton Trans.* **1997**, 4625.
(11) See discussion in ref 2 and (a) Zhou, Y.; Richeson, D. S. *Inorg. Chem.* **1997**, *36*, 501. (b) Hao, S.; Gambarotta, S.; Bensimon, C.; Edema, J. J. H. *Inorg. Chim. Acta* **1993**, *213*, 65. (c) Hao, S.; Berno, P.; Minhas, R. K.; Gambarotta, S. *Inorg. Chim. Acta* **1996**, *244*, 37. (d) Hao, S.; Feghali, K.; Gambarotta, S. *Inorg. Chem.* **1997**, *36*, 1745.
(12) Hausen, H.-D.; Gerstner, F.; Schwartz, W. *J. Organomet. Chem.* **1978**, *145*, 277.
(13) Bear, J. L.; Li, Y.; Han, B.; Kadish, K. M. *Inorg. Chem.* **1996**, *35*, 1395.
(14) Cotton, F. A.; Matonic, J. H.; Murillo, C. A. *J. Am. Chem. Soc.* **1997**, *119*, 7889.
(15) (a) Cotton, F. A.; Daniels, L. M.; Murillo, C. A.; Timmons, D. J. *Chem. Commun.* **1997**, 1449. (b) Cotton, F. A.; Timmons, D. J. *Polyhedron* **1998**, *17*, 179.
(16) The solid-state structure of Li[(^{t}BuN)$_2$CNH^{t}Bu](THF) was reported recently, see: Chivers, T.; Parvez, M.; Schatte, G. *J. Organomet. Chem.* **1998**, *550*, 213.

Table 1. Summary of Crystal Data for Compounds 1a, 1d, and 3

complex	1a	1d	3
formula	$C_9H_{20}AlCl_2N_3$	$C_{13}H_{32}AlCl_2N_3Si_2$	$C_9H_{18}AlN_3$
fw	268.16	384.48	195.24
cryst size, mm	0.56 × 0.06 × 0.28	0.40 × 0.29 × 0.27	0.20 × 0.10 × 0.09
color/shape	colorless/plate	colorless/irreg block	colorless/block
D(calc), Mg/m^3	1.229	1.148	1.234
cryst syst	monoclinic	monoclinic	monoclinic
space group	$P2_1/n$	$C2/c$	$P2_1/n$
a, Å	13.127(3)	14.7523(4)	9.0526(2)
b, Å	8.520(3)	10.9962(1)	11.2782(2)
c, Å	13.432(3)	14.2180(4)	10.4250(1)
β, deg	105.24(2)	105.298(2)	99.135(1)
V, Å^3	1449.4(7)	2224.71(9)	1050.86(3)
Z	4	4	4
temp, K	210(2)	173(2)	173(2)
diffractometer	Enraf-Nonius CAD4	Siemens SMART platform CCD	Siemens SMART platform CCD
radiation, λ (Å)	Mo Kα, 0.710 73	Mo Kα, 0.710 73	Mo Kα, 0.710 73
2θ range, deg	5.0 < 2θ < 50.0	4.7 < 2θ < 50.1	5.4 < 2θ < 50.0
data collected: $h;k;l$	−15,10; −1,10; ±15	−17,16; 0,13; 0,16	±10; 0,13; 0,12
no. of reflns	3718	5433	5816
no. of unique reflns	2514	1939	1842
R_{int}	0.0581	0.0263	0.0301
no. of obsd reflns	$I > 2\sigma(I)$, 1519	$I > 2\sigma(I)$, 1399	$I > 2\sigma(I)$, 1542
μ, mm^{-1}	0.486	0.437	0.153
transmission range, %	78−100	75−100	84−100
data/params	2514/216	1939/102	1842/120
structure solution	direct methods[a]	direct methods[b]	direct methods[b]
GOF on F^2	1.135	1.079	1.059
R indices ($I > 2\sigma(I)$)[c,d]	R1 = 0.0517, wR2 = 0.1124	R1 = 0.0611, wR2 = 0.1457	R1 = 0.0429, wR2 = 0.1004
R indices (all data)[c,d]	R1 = 0.1094, wR2 = 0.1512	R1 = 0.0858, wR2 = 0.1585	R1 = 0.0571, wR2 = 0.1069
max resid density, e/Å^3	0.39	0.52	0.29

[a] *MULTAN, Multan80*; University of York: York, England. [b] *SHELXTL-Plus Version 5*; Siemens Industrial Automation, Inc.: Madison, WI. [c] $R1 = \sum||F_o| - |F_c||/\sum|F_o|$. [d] $wR2 = [\sum[w(F_o^2 - F_c^2)^2]/\sum[w(F_o^2)^2]]^{1/2}$, where $w = q[\sigma^2(F_o^2) + (aP)^2 + bP]^{-1}$.

Table 2. Selected Bond Lengths (Å) and Angles (deg) for 1a

Al(1)−N(1)	1.873(3)	Al(1)−N(2)	1.870(4)
Al(1)−Cl(1)	2.124(2)	Al(1)−Cl(2)	2.113(2)
N(1)−C(3)	1.356(6)	N(2)−C(3)	1.360(5)
N(7)−C(3)	1.343(5)	N(1)−C(4)	1.468(5)
N(2)−C(11)	1.478(6)	N(7)−C(8)	1.461(6)
N(7)−C(9)	1.446(6)		
N(1)−Al(1)−N(2)	72.7(2)	Cl(1)−Al(1)−Cl(2)	109.62(8)
N(1)−Al(1)−Cl(1)	116.4(1)	N(1)−Al(1)−Cl(2)	119.0(1)
N(2)−Al(1)−Cl(1)	118.6(1)	N(2)−Al(1)−Cl(2)	116.7(1)
C(3)−N(1)−Al(1)	89.0(2)	C(3)−N(2)−Al(1)	89.0(3)
N(1)−C(3)−N(2)	109.4(3)	C(4)−N(1)−Al(1)	135.1(3)
C(11)−N(2)−Al(1)	135.0(3)	C(3)−N(1)−C(4)	124.2(3)
C(3)−N(2)−C(11)	124.5(4)	N(1)−C(3)−N(7)	126.2(4)
N(2)−C(3)−N(7)	124.4(4)	C(3)−N(7)−C(8)	121.7(4)
C(3)−N(7)−C(9)	122.6(4)	C(8)−N(7)−C(9)	115.5(4)

Table 3. Selected Bond Lengths (Å) and Angles (deg) for 1d[a]

Al(1)−N(1)	1.878(3)	Al(1)−Cl(1)	2.103(2)
N(1)−C(1)	1.341(4)	C(1)−N(2)	1.400(6)
N(1)−C(2)	1.458(4)	N(2)−Si(1)	1.772(2)
Si−C(average)	1.842(5)		
N(1)−Al(1)−N(1A)	71.4(2)	Cl(1)−Al(1)−Cl(1A)	111.3(1)
N(1)−Al(1)−Cl(1)	117.2(1)	N(1)−Al(1)−Cl(1A)	117.4(1)
C(1)−N(1)−Al(1)	89.4(2)	N(1)−C(1)−N(1A)	109.7(4)
C(2)−N(1)−Al(1)	144.4(2)	C(1)−N(1)−C(2)	126.0(3)
N(1)−C(1)−N(2)	125.2(2)	C(1)−N(2)−Si(1)	117.5(1)
Si(1)−N(2)−Si(1A)	125.1(2)		

[a] Symmetry transformations used to generate equivalent atoms: $-x + 1, y, -z + 1/2$.

crystals. The ^{1}H NMR spectrum of **3** contains three methylene resonances for the hpp$^-$ ligand and a high-field singlet for the Al*Me*$_2$ groups, consistent with a time-averaged D_{2h}-symmetric structure. The highest m/z peak in the EI-mass spectrum of **3** corresponds to the $[\{(\mu\text{-hpp})AlMe_2\}_2 - Me]^+$ ion, which suggests that **3** adopts a dimeric or higher nuclearity structure. The dimeric structure was confirmed by X-ray crystallography (vide infra).

Molecular Structures of {R$_2$NC(N^{i}Pr)$_2$}AlCl$_2$ (1a, R = Me; 1d, R = SiMe$_3$). Crystal data for **1a** and **1d** are summarized in Table 1, refinement details are discussed in the Experimental Section, and selected bond distances and angles are listed in Tables 2 and 3. Molecular geometries and atom-labeling schemes are shown in Figures 1 and 2.

Complexes **1a** and **1d** both adopt monomeric, distorted tetrahedral structures with chelating guanidinate ligands. The guanidinate bite angles (N−Al−N) are acute (**1a** = 72.7°; **1d** = 71.4°) and comparable to the amidinate bite angles in {RC(N^{i}Pr)$_2$}AlCl$_2$ complexes (R = Me, 71.2°; R = ^{t}Bu, 70.6°).[2] The acute N−Al−N angles in **1a** and **1d** are compensated for by large N−Al−Cl angles (117.5° average), while the Cl−Al−Cl

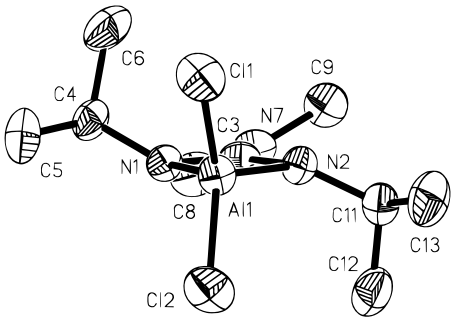

Figure 1. Molecular structure of {Me$_2$NC(N^{i}Pr)$_2$}AlCl$_2$ (**1a**, H-atoms omitted).

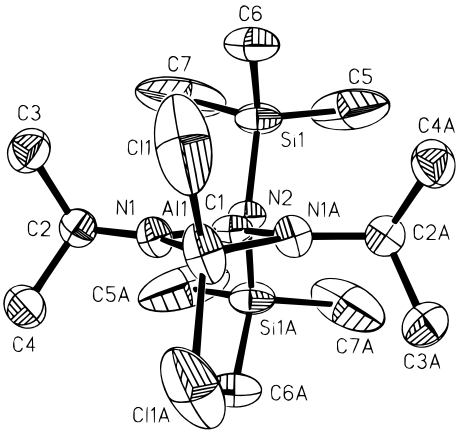

Figure 2. Molecular structure of $\{(Me_3Si)_2NC(N^iPr)_2\}AlCl_2$ (**1d**, H-atoms omitted).

angles (110.4° average) are close to the ideal tetrahedral value. The guanidinate ligands in **1a** and **1d** are symmetrically bound, and the chelate rings are flat (N−Al−N−C torsion angles = 0°, −0.4°). The Al−N and Al−C distances are very similar to the corresponding distances in $\{RC(NR'_2)_2\}AlCl_2$ compounds.

The structures of **1a** and **1d** differ significantly in three respects: (i) in **1a** the CNR_2 plane is rotated 28.4° out of the chelate ring plane (angle between C(8)−N(7)−C(9) and Al(1)−N(1)−C(3)−N(2) planes = 28.4°), while in **1d** the CNR_2 plane is nearly perpendicular to the chelate ring plane (angle between Si(1)−N(2)−Si(1A) and Al(1)−N(1)−C(1)−N(1A) planes = 86.2°), (ii) the C−NR_2 distance in **1a** (C(3)−N(7) = 1.343(5) Å) is shorter than the corresponding distance in **1d** (C(1)−N(2) = 1.400(4) Å), and (iii) in **1a** the C−NR_2 distance is very similar to the average C−NR′ distance (C(3)−N(1), C(3)−N(2) average = 1.358(3) Å), while in **1d** the C−NR_2 distance is longer than the C−NR′ distance (C(1)−N(1) = 1.341(4) Å). Thus, C−NR_2 π-bonding is significant, and resonance structure **F** (Chart 2) makes a major contribution to the guanidinate bonding in **1a** but not in **1d**. In the latter compound, N−Si π-bonding utilizes the $-N(SiMe_3)_2$ lone pair and resonance structures **D** and **E** dominate the guanidinate bonding.[17] Steric crowding between the $SiMe_3$ and ^{i}Pr groups in **1d** also contributes to the preference for the perpendicular orientation of the $-N(SiMe_3)_2$ group, the closest $SiMe_3/^i$Pr H−H contact being 2.3 Å.[18]

Interestingly, despite the greater contribution of resonance structure **F** to the guanidinate bonding in **1a** compared to **1d**, the Al−N distances the two compounds are essentially equal (**1a**, 1.872(3) Å; **1d**, 1.878(3) Å). In **1a**, the donor nitrogens are distinctly pyramidal (sum of angles at N(1) = 348.3°, at N(2) = 348.5°) and the N−^{i}Pr bonds project out of metallacycle plane by an average of 26.3°. This effect probably arises from steric crowding between the ^{i}Pr and NMe_2 groups as there are several close H−H contacts (2.2 Å) between these

(17) (a) The N(2)−Si(1) distance in **1d** (1.772(2) Å) is longer than that in $MeN(SiMe_3)_2$ (1.719(4) Å) and the $CNSi_2$ framework is planar (sum of angles around N(2) = 360.0°). The slight lengthening of the N−Si bonds in **1d** versus $MeN(SiMe_3)_2$ probably reflects steric crowding. The Si-N−Si angle in **1d** (125.1(2)°) is smaller than that in $MeN(SiMe_3)_2$ (129.4(6)°). (b) Rankin, D. W. H.; Robertson, H. E. *J. Chem. Soc., Dalton Trans.* **1987**, 785.

(18) Close H−H contacts: H(6A)−H(3A) = 2.3 Å; H(7C)−H(2A) = 2.5 Å. Sum of van der Waals radii = 2.4 Å.

Table 4. Selected Bond Lengths (Å) and Angles (deg) for 3[a]

Al(1)−N(1)	1.916(2)	Al(1)−N(2A)	1.920(2)
Al(1)−C(8)	1.985(2)	Al(1)−C(9)	1.993(2)
N(1)−C(7)	1.348(3)	N(2)−C(7)	1.346(3)
N(3)−C(7)	1.357(3)	N(1)−C(1)	1.474(3)
N(2)−C(6)	1.471(3)	N(3)−C(3)	1.469(3)
N(3)−C(4)	1.468(3)		
N(1)−Al(1)−N(2A)	110.14(8)	C(8)−Al(1)−C(9)	111.0(1)
N(1)−Al(1)−C(8)	112.37(9)	N(1)−Al(1)−C(9)	105.96(9)
N(2A)−Al(1)−C(8)	110.49(9)	N(2A)−Al(1)−C(9)	106.64(9)
C(7)−N(1)−Al(1)	122.2(2)	C(7)−N(2)−Al(1A)	120.3(2)
N(1)−C(7)−N(2)	118.3(2)	C(1)−N(1)−Al(1)	121.1(1)
C(6)−N(2)−Al(1A)	119.7(1)	C(1)−N(1)−C(7)	114.5(2)
C(6)−N(2)−C(7)	114.7(2)	N(1)−C(7)−N(3)	120.9(2)
N(2)−C(7)−N(3)	120.9(2)	C(3)−N(3)−C(7)	123.8(2)
C(4)−N(3)−C(7)	123.8(2)	C(3)−N(3)−C(4)	112.4(2)

[a] Symmetry transformations used to generate equivalent atoms: $-x, -y + 1, -z + 2$.

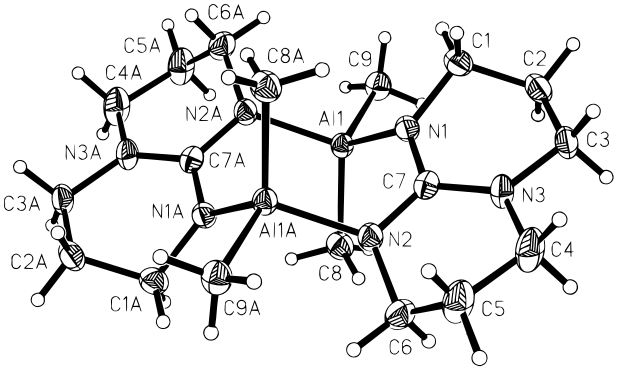

Figure 3. Molecular structure of $\{(\mu\text{-hpp})AlMe_2\}_2$ (**3**).

groups.[19] The pyramidal geometry at N(1) and N(2) implies that there is partial localization of lone-pair electron density at these nitrogens (i.e., partial sp^3 character), and thus, the expected enhancement of Al−N bonding due to the increased charge on the donor nitrogens is not realized. In **1d**, however, the donor nitrogen atoms (N(1), N(1A)) have a distorted trigonal-planar geometry (sum of angles ca. 359.8°) and the N−^{i}Pr bonds lie in the metallacycle plane.

Molecular Structure of $\{(\mu\text{-hpp})AlMe_2\}_2$ (3). Crystal data for **3** are summarized in Table 1, refinement details are discussed in the Experimental Section, and selected bond distances and angles are listed in Table 4. Molecular geometries and atom-labeling schemes are shown in Figure 3.

Complex **3** adopts a dimeric structure in which the bridging hpp^- ligands link the two $AlMe_2$ units in an eight-membered ring with a chair conformation. Overall, the structure of **3** is very similar to that of the dimeric μ-amidinate complex $[\{\mu\text{-}MeC(NMe_2)_2\}AlMe_2]_2$.[12] The geometry at the aluminum atoms is close to tetrahedral, with interligand angles in the range 106.0−112.4°. In particular, the C(8)−Al(1)−C(9) angle (111.0(1)°) is significantly smaller than the corresponding angles in $\{MeC(NCy)_2\}AlMe_2$ (118.6(2)°) and $\{^tBuC(NCy)_2\}AlMe_2$ (116.2(1)°).[2] The Al−N distances (1.918(3) Å average) are ca. 0.05 Å longer than those in the dichloride complexes **1a** and **1d**, as expected due to the greater electron-donating ability of Me vs Cl, but are

(19) Close H−H contacts: H(8A)−H(4A) = 2.2 Å; H(9A)−H(11A) = 2.2 Å; H(8C)−H(4A) = 2.4 Å; H(9B)−H(11A) = 2.4 Å.

very similar to those in $\{MeC(NCy)_2\}AlMe_2$ (1.924(3) Å average) and $[\{\mu\text{-}MeC(NMe_2)_2\}AlMe_2]_2$ (1.926(3) Å).[2,12] The bond distances within the planar CN_3 core of **3** are intermediate between the corresponding distances of **1a** and **1d**. However, the angle between the N(1)−C(7)−N(2) and C(3)−N(3)−C(4) planes of **3** (8.0°) is smaller than the corresponding angles of **1a** (28.4°) and **1d** (86.2°). Comparison of the bonding in the guanidinate core of **3** to that in **1a** and **1d** is complicated by the bicyclic structure of the hpp⁻ ligand and the difference in guanidinate bonding mode (bridging versus chelating) of these compounds.

Conclusions

This work establishes that (i) aluminum complexes containing a variety of guanidinate ligands are accessible by the reaction of in-situ-generated $Li[R_2NC(NR')_2]$ salts with $AlCl_3$ or $AlMe_2Cl$ or alternatively by alkane elimination reactions, (ii) the molecular structures of monomeric $\{R_2NC(NR')_2\}AlCl_2$ complexes are very similar to those of $\{RC(NR')_2\}AlX_2$ amidinate compounds, (iii) the structure of and charge distribution in the $\{R_2NC(NR')_2\}Al$ cores of monomeric $\{R_2NC(NR')_2\}AlX_2$ complexes are very sensitive to steric and π-bonding effects, which influence the extent of delocalization within the guanidinate ligand and the orientation of the donor −NR′ groups, and (iv) the geometry at Al in $\{(\mu\text{-hpp})AlMe_2\}_2$ is much less distorted from tetrahedral than in monomeric $\{R_2NC(NR')\}AlCl_2$ or $\{RC(NR')_2\}AlX_2$ complexes due to the μ-guanidinate bonding, which is enforced by the bicyclic structure of the hpp⁻ ligand. Our future reports will describe how these structural and electronic trends influence the reactivity of cationic aluminum guanidinate compounds.[20]

Experimental Section

General Procedures. All manipulations were performed on a high-vacuum line or in a glovebox under a purified N_2 atmosphere. Solvents were distilled from Na/benzophenone ketyl, except for chlorinated solvents, which were distilled from activated molecular sieves (3 Å) or CaH_2. All other chemicals were purchased from Aldrich and used as received. NMR spectra were recorded on a Bruker AMX 360 spectrometer in sealed or Teflon-valved tubes at ambient probe temperature unless otherwise indicated. ^1H and ^{13}C chemical shifts are reported versus $SiMe_4$ and were determined by reference to the residual ^1H and ^{13}C solvent peaks. Coupling constants are reported in hertz. Mass spectra were obtained using the direct insertion probe method on a VG Analytical Trio I instrument operating at 70 eV. Melting point determinations were performed on samples which were sealed under vacuuum. Elemental analyses were performed by Desert Analytics Laboratory (Tuscon, AZ).

$\{Me_2NC(N^iPr)_2\}AlCl_2$ (1a). A slurry of $LiNMe_2$ (0.765 g, 15.0 mmol) in Et_2O (25 mL) was cooled to 0 °C, and a solution of 1,3-diisopropylcarbodiimide (1.89 g, 15.0 mmol) in Et_2O (15 mL) was added dropwise. The resulting mixture was allowed to warm to room temperature and stirred for 1 h. The mixture was cooled to −78 °C, and a solution of $AlCl_3$ (2.00 g, 15.0 mmol) in Et_2O (15 mL) was added dropwise. The resulting mixture was allowed to warm to room temperature and stirred for 18 h. The volatiles were removed under vacuum, and the product was extracted from the LiCl with toluene. The toluene extract was concentrated and cooled to −30 °C to yield clear, colorless crystals, which were isolated by filtration (2.20 g, 55% based on $AlCl_3$). ^1H NMR (CD_2Cl_2): δ 3.56 (sept, $^3J_{HH} = 6.3$, 2H, C*H*Me$_2$, 2.96 (s, 6H, N*Me*$_2$), 1.12 (d, $^3J_{HH} = 6.1$, 12H, CH*Me*$_2$). ^{13}C NMR (CD_2Cl_2): δ 169.1 (s, *C*N$_3$), 45.7 (d, $^1J_{CH} = 138$, *C*HMe$_2$), 39.5 (q, $^1J_{CH} = 140$, N*Me*$_2$), 23.9 (q, $^1J_{CH} = 125$, CH*Me*$_2$). Mp 85−88 °C. Anal. Calcd for $C_9H_{20}AlCl_2N_3$: C, 40.31; H, 7.52; N, 15.67. Found: C, 40.36; H, 7.74; N, 15.39. MS (EI, *m*/*z*, ^{35}Cl): 267 $[M]^+$, 252 $[M - Me]^+$.

$\{Et_2NC(N^iPr)_2\}AlCl_2$ (1b). This compound was prepared by the procedure outlined for **1a**, using 1.19 g of $LiNEt_2$ (15.0 mmol), 1.89 g of 1,3-diisopropylcarbodiimide (15.0 mmol), and 2.00 g of $AlCl_3$ (15.0 mmol). This complex was isolated as clear, colorless crystals (3.01 g, 68% based on $AlCl_3$). ^1H NMR (CD_2Cl_2): δ 3.46 (sept, $^3J_{HH} = 6.4$, 2H, C*H*Me$_2$), 3.33 (q, $^3J_{HH} = 7.1$, 4H, C*H*$_2$Me), 1.19 (t, $^3J_{HH} = 6.7$, 6H, CH$_2$*Me*), 1.14 (d, $^3J_{HH} = 6.1$, 12H, CH*Me*$_2$). ^{13}C NMR (CD_2Cl_2): δ 168.8 (s, *C*N$_3$), 45.8 (d, $^1J_{CH} = 137$, *C*HMe$_2$), 43.1 (t, $^1J_{CH} = 136$, *C*H$_2$Me), 24.1 (q, $^1J_{CH} = 127$, CH*Me*$_2$), 12.9 (q, $^1J_{CH} = 127$, CH$_2$*Me*). Mp: 94−97 °C. Anal. Calcd for $C_{11}H_{24}N_3AlCl_2$: C, 44.60; H, 8.17; N, 14.19. Found: C, 44.38; H, 7.89; N, 14.04. MS (EI, *m*/*z*, ^{35}Cl): 295 $[M]^+$, 280 $[M - Me]^+$.

$\{^iPr_2NC(N^iPr)_2\}AlCl_2$ (1c). This compound was prepared by the procedure outlined for **1a**, using 1.61 g of LiN^iPr_2 (15.0 mmol), 1.89 g of 1,3-diisopropylcarbodiimide (15.0 mmol), and 2.00 g of $AlCl_3$ (15.0 mmol). This complex was isolated as pale yellow crystals (1.99 g, 41% based on $AlCl_3$). ^1H NMR (CD_2Cl_2): δ 3.77 (sept, $^3J_{HH} = 6.8$, 2H, C*H*Me$_2$), 3.55 (sept, $^3J_{HH} = 6.2$, 2H, C*H*Me$_2$), 1.37 (d, $^3J_{HH} = 6.8$, 12H, CH*Me*$_2$), 1.18 (d, $^3J_{HH} = 5.8$, 12H, CH*Me*$_2$). ^{13}C NMR (CD_2Cl_2): δ 172.5 (s, *C*N$_3$), 51.1 (d, $^1J_{CH} = 136$, *C*HMe$_2$), 45.9 (d, $^1J_{CH} = 135$, *C*HMe$_2$), 24.7 (q, $^1J_{CH} = 125$, CH*Me*$_2$), 23.5 (q, $^1J_{CH} = 125$, CH*Me*$_2$). Mp: 104−107 °C. Anal. Calcd for $C_{13}H_{28}AlCl_2N_3$: C, 48.15; H, 8.70; N, 12.96. Found: C, 47.87; H, 8.68; N, 12.96. MS (EI, *m*/*z*, ^{35}Cl): 323 $[M]^+$.

$\{(Me_3Si)_2NC(N^iPr)_2\}AlCl_2$ (1d). This compound was prepared by the procedure outlined for **1a**, using 2.00 g of $LiN(SiMe_3)_2$ (12.0 mmol), 1.51 g of 1,3-diisopropylcarbodiimide (12.0 mmol), and 1.59 g of $AlCl_3$ (12.0 mmol). The complex was extracted and recrystallized with pentane and isolated as white crystals (1.41 g, 31% based on $AlCl_3$). ^1H NMR (CD_2Cl_2): δ 3.60 (sept, $^3J_{HH} = 6.6$, 2H, C*H*Me$_2$), 1.14 (d, $^3J_{HH} = 6.5$, 12H, CH*Me*$_2$), 0.30 (s, 18H, Si*Me*$_3$). ^{13}C NMR (CD_2Cl_2): δ 172.4 (s, *C*N$_3$), 44.5 (d, $^1J_{CH} = 134$, *C*HMe$_2$), 25.3 (q, $^1J_{CH} = 124$, CH*Me*$_2$), 2.0 (q, $^1J_{CH} = 119$, Si*Me*$_3$). Mp: 133−135 °C. Anal. Calcd for $C_{13}H_{32}AlCl_2N_3Si_2$: C, 40.61; H, 8.39; N, 10.93. Found: C, 40.44; H, 8.24; N, 10.72. MS (EI, *m*/*z*, ^{35}Cl): 368 $[M - Me]^+$.

$\{Me_2NC(N^iPr)_2\}AlMe_2$ (2a). This compound was prepared by the procedure outlined for **1a**, using 0.809 g of $LiNMe_2$ (15.9 mmol), 2.00 g of 1,3-diisopropylcarbodiimide (15.9 mmol), and 1.47 mL of $AlMe_2Cl$ (15.9 mmol). The complex was extracted using pentane, and the volatiles were removed under vacuum, yielding the crude product as a sticky yellow solid. Clear, colorless crystals were obtained by vacuum sublimation at 60 °C onto a dry ice cooled probe (2.2 g, 61% based on $AlMe_2Cl$). Because **2a** is a liquid at room temperature, a small aluminum pan was positioned beneath the cold probe of the sublimator to collect the sublimed product as it melted. ^1H NMR (CD_2Cl_2): δ 3.50 (sept, $^3J_{HH} = 6.3$, 2H, C*H*Me$_2$), 2.85 (s, 6H, N*Me*$_2$), 1.02 (d, $^3J_{HH} = 6.1$, 12H, CH*Me*$_2$), −0.82 (s, 6H, Al*Me*$_2$). ^{13}C NMR (CD_2Cl_2): δ 167.6 (s, *C*N$_3$), 45.2 (d, $^1J_{CH} = 135$, *C*HMe$_2$), 39.2 (q, $^1J_{CH} = 136$, N*Me*$_2$), 24.3 (q, $^1J_{CH} = 125$, CH*Me*$_2$), −8.7 (q, $^1J_{CH} = 110$ Al*Me*$_2$). Mp: 30−32 °C. Anal. Calcd for $C_{11}H_{26}AlN_3$: C, 58.12; H, 11.53; N, 18.48. Found: C, 57.97; H, 11.70; N, 18.25. MS (EI, *m*/*z*): 212 $[M - Me]^+$.

$\{Et_2NC(N^iPr)_2\}AlMe_2$ (2b). This compound was prepared by the procedure outlined for **1a**, using 1.25 g of $LiNEt_2$ (15.9 mmol), 2.00 g of 1,3-diisopropylcarbodiimide (15.9 mmol), and

(20) While this work was in review, Chang et al. reported the synthesis of several aluminum guanidinate compounds by a different method, see: Chang, C.; Hsiung, C.; Su, H.; Srinivas, B.; Chiang, M. Y.; Lee, G.; Wang, Y. *Organometallics* **1998**, *17*, 1595.

1.47 mL of $AlMe_2Cl$ (15.9 mmol). The complex was extracted with pentane, and the volatiles were removed under vacuum, yielding the crude product as a sticky orange solid. Clear, colorless crystals (2.39 g, 59% based on $AlMe_2Cl$) were isolated by vacuum sublimation at 70 °C onto a dry ice cooled probe. ^{1}H NMR (CD_2Cl_2): δ 3.41 (sept, $^3J_{HH} = 6.3$, 2H, C*H*Me$_2$), 3.21 (q, $^3J_{HH} = 7.3$, 4H, C*H*$_2$Me), 1.14 (t, $^3J_{HH} = 7.2$, 6H, CH$_2$*Me*), 1.03 (d, $^3J_{HH} = 6.5$, 12H, CH*Me*$_2$), −0.82 (s, 6H, Al*Me*$_2$). ^{13}C NMR (CD_2Cl_2): δ 167.3 (s, *C*N$_3$), 45.3 (d, $^1J_{CH} = 135$, *C*HMe$_2$), 42.6 (t, $^1J_{CH} = 136$, *C*H$_2$Me), 24.6 (q, $^1J_{CH} = 126$, CH*Me*$_2$), 13.2 (q, $^1J_{CH} = 126$, CH$_2$*Me*), −8.6 (q, $^1J_{CH} = 112$, Al*Me*$_2$). Mp: 26.5−28 °C. Anal. Calcd for $C_{13}H_{30}AlN_3$: C, 61.14; H, 11.84; N, 16.45. Found: C, 60.88; H, 11.97; N, 16.30. MS (EI, *m*/*z*): 240 [M − Me]$^+$.

{^{i}Pr$_2$NC(N^{i}Pr)$_2$}AlMe$_2$ (2c). This compound was prepared by the procedure outlined for **1a**, using 4.24 g of Li*N*^{i}Pr$_2$ (39.6 mmol), 5.00 g of 1,3-diisopropylcarbodiimide (39.6 mmol), and 3.68 mL of $AlMe_2Cl$ (39.6 mmol). The product was isolated as a reddish-brown liquid from which white crystals were obtained by recrystallization from pentane in a −78 °C cold bath (5.26 g, 46.8% yield based on $AlMe_2Cl$). Analytically pure, waxy, white crystals were obtained by vacuum sublimation at 65 °C onto a dry ice cooled probe (2.54 g, 23% yield based on $AlMe_2Cl$). ^{1}H NMR (CD_2Cl_2): δ 3.59 (sept, $^3J_{HH} = 5.7$, 2H, C*H*Me$_2$), 3.52 (sept, $^3J_{HH} = 6.0$, 2H, C*H*Me$_2$), 1.22 (d, $^3J_{HH} = 7.2$, 12H, CH*Me*$_2$), 1.04 (d, $^3J_{HH} = 6.1$, 12H, CH*Me*$_2$), −0.81 (s, 6H, Al*Me*$_2$). ^{13}C NMR (CD_2Cl_2): δ 168.1 (s, *C*N$_3$), 49.1 (d, $^1J_{CH} = 132$, *C*HMe$_2$), 45.0 (d, $^1J_{CH} = 133$, *C*HMe$_2$), 25.5 (q, $^1J_{CH} = 125$, CH*Me*$_2$), 23.3 (q, $^1J_{CH} = 126$, CH*Me*$_2$), −9.4 (q, $^1J_{CH} = 115$, Al*Me*$_2$). Mp: 48−49.5 °C. Anal. Calcd for $C_{15}H_{34}AlN_3$: C, 63.56; H, 12.09; N, 14.83. Found: C, 63.14; H, 12.29; N, 14.44. MS (EI, *m*/*z*): 268 [M − Me]$^+$.

{(*μ*-hpp)AlMe$_2$}$_2$ (3). A solution of $AlMe_3$ (1.04 g, 14.4 mmol) in hexanes (20 mL) was added to a suspension of 1,3,4,6,7,8-hexahydro-2*H*-pyrimido[1,2-*a*]pyrimidine (hppH) (2.00 g, 14.4 mmol) in hexanes (80 mL). An exothermic reaction was observed, and a gas was evolved. After 18 h, the volatiles were removed under vacuum to afford {(*μ*-hpp)-AlMe$_2$}$_2$ as a white solid (2.10 g, 75%). This compound was purified by dissolving the crude sample in hot (60 °C) THF and subsequent crystallization at −30 °C. ^{1}H NMR (C_7D_8): δ 3.06 (m, 4H, C*H*$_2$), 2.43 (t, $^3J_{HH} = 6.8$, 4H, C*H*$_2$), 1.51 (m, 4H, C*H*$_2$), −0.46 (s, 6H, Al*Me*$_2$). ^{13}C NMR (C_7D_8): δ 163.1 (s, *C*N$_3$), 47.8 (t, $^1J_{CH} = 135$, *C*H$_2$), 41.1 (t, $^1J_{CH} = 138$, *C*H$_2$), 24.4 (t, $^1J_{CH} = 130$, CH$_2$), −8.3 (br q, Al*Me*$_2$). Anal. Calcd for $C_9H_{18}AlN_3$: C, 55.37; H, 9.29; N, 21.52. Found: C, 54.84; H, 9.25; N, 21.24. MS (EI, *m*/*z*): 375 [M − Me]$^+$.

X-ray Crystallography. The structure of **1a** was determined at the University of Iowa by D. C. Swenson. The structures of **3** and **1d** were determined at the University of Minnesota by V. G. Young, Jr. Crystal data, data collection details, and solution and refinement procedures are collected in Table 1. Additional comments specific to each structure follow.

{Me$_2$NC(N^{i}Pr)$_2$}AlCl$_2$ (**1a**): crystals were obtained by recrystallization from pentane at −30 °C. All non-H atoms were refined with anisotropic thermal parameters, and H-atoms were refined with isotropic thermal parameters.

{(Me$_3$Si)$_2$NC(N^{i}Pr)$_2$}AlCl$_2$ (**1d**): crystals were obtained by recrystallization from pentane at −30 °C. All non-H atoms were refined anisotropically, and all H-atoms were placed in ideal positions and refined as riding atoms with group isotropic displacement parameters. Thermal ellipsoid diagrams reveal a great deal of thermal motion pivoting about the center of mass situated in the vicinity of C(1). Cl(1) and Al(1) have similar thermal ellipsoids, but Al(1) should reside on the crystallographic 2-fold axis. The thermal motion of Al(1) suggested that other models should be examined. A model in *C*2/*c* with partial occupancies for Cl(1) and Al(1) and an alternative model in *Cc* with one complete molecule in a racemic twin were examined. Both models diverged, and thus, the original model was considered correct. Examination of the packing diagram may explain the unusual thermal motion. The bulky $AlCl_2$ unit fits directly behind the N(SiMe$_3$)$_2$ moiety of an adjacent molecule on the crystallographic 2-fold axis, and thus, no H-bonds are possible. The average structure conforms to the *C*2/*c* model.

{(*μ*-hpp)AlMe$_2$}$_2$ (**3**): crystals were obtained by recrystallization from THF at −30 °C. All non-H atoms were refined anisotropically, and all H-atoms were placed in ideal positions and refined as riding atoms with group isotropic displacement parameters.

Acknowledgment. This work was supported by DOE Grant No. DE-FG02-88ER13935. M.P.C. was supported in part by a NATO postdoctoral research fellowship.

Supporting Information Available: Tables of atomic coordinates, isotropic displacement parameters, anisotropic displacement parameters, bond distances and bond angles, and hydrogen atom coordinates (13 pages). Ordering information is given on any current masthead page.

OM980223M